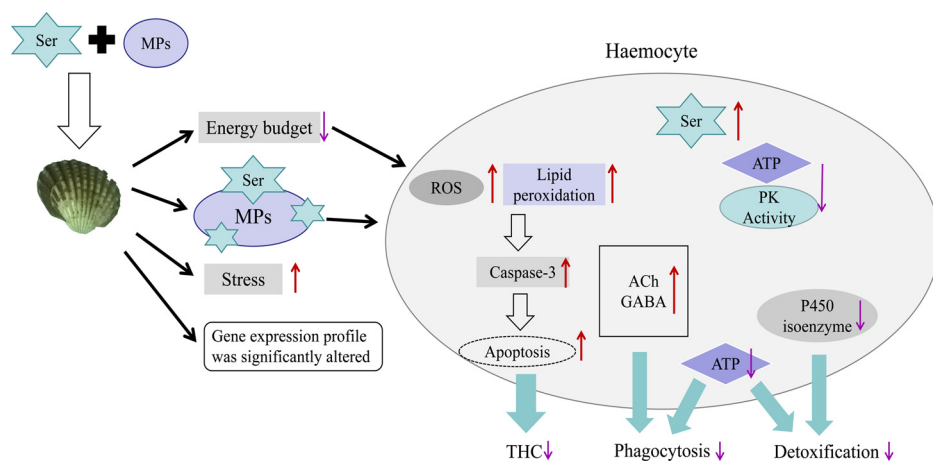ELSEVIER

Immunotoxicities of microplastics and sertraline, alone and in combination, to a bivalve species: size-dependent interaction and potential toxication mechanism

Wei Shi[1], Yu Han[1], Shuge Sun, Yu Tang, Weishang Zhou, Xueying Du, Guangxu Liu*

College of Animal Sciences, Zhejiang University, Hangzhou, PR China

GRAPHICAL ABSTRACT

ARTICLE INFO

ABSTRACT

Although coexposure to pharmaceuticals and microplastics (MPs) may frequently occur, the synergistic impact of MPs and antidepressants on marine species still remains poorly understood. In this study, the immunotoxicities of polystyrene MPs (diameters 500 nm and 30 μm) and sertraline (Ser), alone and in combination, were investigated in a bivalve mollusk *Tegillarca granosa*. Results showed that both MPs and Ser significantly suppressed the immune responses of *T. granosa*. In addition, though the toxic effect of Ser was not affected by microscale MPs, an evident synergistic immuno-toxic effect was observed between Ser and nanoscale MPs, which indicates a size-dependent interaction between the two. To further ascertain the underlying toxication mechanisms, the intracellular content of reactive oxygen species, apoptosis status, ATP content, pyruvate kinase activity, plasma cortisol level, and *in vivo* concentrations of neurotransmitters and cytochrome P450 1A1 were analysed. A transcriptomic analysis was also performed to reveal global molecular alterations following Ser and/or MPs exposure. The obtained results indicated that the presence of nanoscale MPs may enhance the immunotoxicity of Ser by (i) inducing apoptosis of haemocytes and, hence, reducing the THC; (ii) constraining the energy availability for phagocytosis; and (iii) hampering the detoxification of Ser.

---

* Corresponding author.
    E-mail addresses: guangxu_liu@qq.com, guangxu_liu@zju.edu.cn (G. Liu).
    [1] These authors contributed equally to this manuscript.

1. Introduction

Approximately 7000 million tons of plastic waste has been generated globally since the 1950s, which has become a global environmental problem (Jambeck et al., 2015). Currently, plastics are commonly found in various oceanic compartments, including polar areas and abyssal regions, a significant part of which is composed of particles with diameters smaller than 5 mm, which are defined as microplastics (MPs) (Andrady, 2011; Van Cauwenberghe et al., 2015). According to estimation, the total amount of MPs in the world's oceans is in the range of 15 to 51 trillion pieces, which may pose a significant threat to marine species and the entire ecosystem (Van Sebille et al., 2015).

As reported in previous studies, MPs can be easily consumed by various marine organisms (Li et al., 2015; Van Cauwenberghe et al., 2015), and thus exerting adverse effects on various aspects of these organisms, such as the embryonic development retardation (Sussarellu et al., 2016), nutritional disturbance (Barnes et al., 2009; Yin et al., 2018), growth arrest (Besseling et al., 2014), and immune suppression (Tang et al., 2020). Owing to the larger specific surface area, MPs can impact organisms not only directly through their inherent properties, but also indirectly by acting as transport vectors for other harmful pollutants (Rochman et al., 2014; Brennecke et al., 2016; Lu et al., 2018). Far worse, increasing evidence suggests MPs can even alter the toxicity of other contaminants (Sleight et al., 2017). However, the molecular mechanisms behind such interactions between MPs and other pollutants are still unknown in marine species.

Owing to the large increase in the production and consumption of pharmaceuticals over the past few decades, the release of pharmaceutical compounds into the marine environment constitutes a cause for great public concern, considering the potential threat they pose to various marine organisms (Franzellitti et al., 2014; Silva et al., 2015; Shi et al., 2019). Antidepressants are currently one of the most widely prescribed subsets of pharmaceuticals, the consumption of which has doubled in Organisation for Economic Cooperation and Development (OECD) countries from 2000 to 2015 (OECD, 2017). Accordingly, an increasing number of studies have demonstrated the presence of antidepressants in various aquatic systems (Schultz et al., 2010; Silva et al., 2015). Although they have been specifically designed for humans, more and more data suggest that antidepressants, even at environmentally relevant trace concentration, may threaten the reproduction, development, behaviour, and survival of various aquatic organisms (Christen et al., 2010; Silva et al., 2015). However, the toxication mechanisms of antidepressants are still unclear in aquatic species, let alone their interactions with other waterborne contaminants (Silva et al., 2015; Miller et al., 2018).

Various sessile benthic bivalves, living in proximity to sediments of coastal and estuary areas, may be simultaneously exposed to high concentrations of MPs and antidepressants (Graca et al., 2017; Li et al., 2019; Tang et al., 2020). First, in hydrochloride salt forms, many antidepressants have low octanol/water partition coefficients (K_{ow}) and relatively high coefficients of sorption (K_{oc}) to sediments, which leads to a higher concentration in the water-sediment interface area (Kwon & Armbrust, 2006; Furlong et al., 2004; Sánchez-Argüello et al., 2009). Second, coastal and estuary areas with mass industries and agricultural activities are also major sinks for MPs (Lozoya et al., 2016). Furthermore, in addition to ingesting MPs suspended in seawater, benthic suspension feeders including bivalves may also be susceptible to sinking MP particles (Van Cauwenberghe et al., 2015). The high coexposure risk highlights the need to elucidate the impacts of the MP-antidepressant coexposure on benthic bivalves.

Maintaining a robust immune response is crucial for the survivorship of bivalve species in the complex marine environment (Liu et al.,

2016; Guan et al., 2019). However, the immune system of bivalves is considered as one of the main targets for various pollutants including antidepressants and MPs (Avio et al., 2015; Détrée and Gallardo-Escárate, 2018; Shi et al., 2019). In addition, recent studies suggest that antidepressants may interact with MPs in the water environment and lead to altered toxicity to aquatic organisms (Razanajatovo et al., 2018; Qu et al., 2019). Nevertheless, to the best of our knowledge, the combined effects of MPs and antidepressants on the immune responses of marine organisms are still unknown.

The blood clam, *T. granosa*, is a traditional aquaculture bivalve species widely distributed throughout the Indo-Pacific region (Han et al., 2019). Since the inhabitation of the intertidal mudflat, where pollutants such as MPs and pharmaceuticals are often concentrated (Graca et al., 2017; Li et al., 2019), the blood clam may be simultaneous under the threat of MPs and pharmaceuticals. Therefore, in this study, to improve the present understanding of the ecotoxicological effects of the MPs and pharmaceuticals, the impacts of PS MPs, one of the most abundant MPs in the marine environment (Browne et al., 2011; Sussarellu et al., 2016), sertraline (Ser), one of the most widely prescribed antidepressants (Schultz et al., 2010), and their combination on the immune responses were investigated in *T. granosa*. In addition, to reveal the toxication mechanisms underpinning, the generation of reactive oxygen species (ROS), lipid peroxidation (determined as malondialdehyde (MDA) content), and apoptosis status (indicated by the caspase-3 activity) of the haemocytes upon MP and/or Ser exposure were analysed. As the phagocytosis of foreign materials by haemocytes is an energy-consuming process (Turvey & Broide, 2010), the impacts of MP and/or Ser exposure on the adenosine triphosphate (ATP) content and pyruvate kinase (PK) activity in haemocytes were assessed. The plasma cortisol levels and *in vivo* concentration of cytochrome P450 1A1 (CYP1A1) were also evaluated as indicators of physiological stress and detoxification activity (Eames et al., 2010; Nash et al., 2014), respectively. Moreover, the impacts of MP and/or Ser exposure on the concentrations of two immune-modulatory neurotransmitters (Liu et al., 2017), acetylcholine (ACh) and γ-aminobutyric acid (GABA), were determined. A transcriptomic analysis was also performed to reveal the possible underlying molecular toxication mechanism.

2. Materials and Methods

2.1. Experimental animals

Adult blood clams *T. granosa* (shell length 23.2 ± 2.7 mm, mean ± SE) were collected in May 2019 from Yueqing Bay (28° 280' N and 121°110' E), Wenzhou, China. Local seawater was sampled and analysed by a high-performance liquid chromatography (HPLC) assay with fluorescence detection (1200 series, Agilent, Germany) following the methods of previous studies (Melis et al., 2012) to obtain the background concentration of Ser, which was determined to be lower than the detection limit (< 10 ng/mL). After cleaning off epibionts on their shells, the clams were transported to the Zhejiang Mariculture Research Institute and acclimated in a 2000 L indoor tank with sand-filtered seawater (temperature 22.1 ± 0.7 °C, pH 8.07 ± 0.08, salinity 20.7 ± 0.6 ‰) under continuous aeration for 14 days. During this period, the clams were fed with microalgae *Platymonas subcordiformis* at a rate of 5 % of the tissue dry weight twice a day and the seawater was replaced daily.

2.2. Chemicals

Ser hydrochloride (CAS # 79559-97-0, purity ≥ 98 %) was obtained from the National Institutes for Food and Drug Control (Beijing,

China). A stock solution of Ser at a dose of 100 mg/L was prepared by dissolving the Ser powder in 1 μm-sieve filtered seawater. PS microbeads (25 mg/mL) with nominal sizes of 500 nm and 30 μm were purchased from Aladdin Reagent Co. Ltd (Shanghai, China). These microbeads were monodisperse and supplied in 10 mL aqueous suspensions without additives. The morphology and sizes of MPs were verified with transmission electron microscopy (TEM, JEM-1230, JEOL, Japan).

2.3. Exposure experiment and sampling

In order to investigate the effects of Ser, MPs, and their combination on *T. granosa*, one control group and five treatment groups were conducted. Blood clams reared in seawater without Ser and MPs were used as a control. Exposure to nanoscale (diameter 500 nm) and microscale (diameter 30 μm) MPs were carried out to obtain MP-exposed groups. Exposure to Ser (100 ng/L) were adopted as a Ser-exposed group. Clam individuals treated with Ser (100 ng/L) and 500 nm or 30 μm MPs were performed as coexposure groups. According to previous studies, a dose of 100 ng/L of Ser was used in this study to simulate the Ser concentration in polluted areas (Kolpin et al., 2002; Salgado et al., 2011). According to the prediction of global plastic waste input and mass concentration of MPs in polluted areas (Goldstein et al., 2012; Jambeck et al., 2015), a concentration of PS microbeads at 0.29 mg/L was chosen to simulate the realistic scenario of MPs in the marine environment. In addition, MPs with two different sizes (diameter 500 nm and 30 μm) with significant differences in their impacts and interactions with other pollutants were assessed in this study to evaluate any size-dependent effect (Chen et al., 2017; Tang et al., 2020). Generally, after the acclimatisation, 720 clam individuals were randomly divided into 18 tanks (6 groups × 3 replicates, 40 clams per tank) containing 40 L of seawater (temperature 23.1 ± 0.3 °C, pH 8.05 ± 0.02, salinity 20.5 ± 0.4 ‰) with corresponding doses and/or sizes of Ser and/or MPs. During this period, the clams were fed with *P. subcordiformis* as described above and seawater was changed daily with Ser and/or MPs freshly added at the corresponding doses and/or sizes. The experiment lasted 14 days; no individual mortality was observed throughout this period.

After the exposure, 81 clam individuals were collected from each treatment group. Haemolymph was extracted from each individual following the method of Liu et al. (2016) and pooled in nine samples (n = 9, each with haemolymph from nine individuals) for the analysis of haemolymph-related parameters. The digestive glands of these clams were dissected on ice, pooled in nine samples (n = 9), and immediately frozen in liquid nitrogen for the analysis of CYP1A1, which is one of the most important xenobiotic metabolism enzymes. Similarly, haemolymph extracted individually from six clams out of each treatment group (n = 6) was used to quantify the contents of plasma cortisol. In addition, digestive glands of 27 clams from each experimental group were peeled off on ice, pooled in three samples (n = 3, each with digestive gland from nine clams), and used for transcriptome sequencing due to their important role in immune functions and as a significant target for both MPs and pharmaceuticals toxicity (Canesi et al., 2007; Avio et al., 2015).

2.4. Analysis of the total counts of haemocytes (THC)

The THC was determined according to the reported methods (Su et al., 2018). Briefly, 100 μL of haemolymph was added into a 1.5 mL centrifuge tube pre-filled with 100 μL of 2.5% glutaraldehyde on ice. After dilution with 900 μL of phosphate buffer saline (PBS, 0.1 M, pH 7.4) and fixation, a wet mount of haemolymph was prepared and examined under an Olympus BX53 microscope (Olympus, Japan) at a magnification of 200 ×. The THC was estimated microscopically in a Neubauer haemocytometer (XB-K-25, Anxin Optical Instrument, China).

2.5. Analysis of phagocytosis

Phagocytosis assays were conducted following the methods reported by Liu et al (2016) and Shi et al (2017). In brief, 100 μL of haemolymph was mixed (1:1) with Alsever's solution (R1016, Solarbio, China) in a 1.5 mL centrifuge tube. Subsequently, rapid determination of the haemocyte concentration was carried out under an Olympus BX53 microscope. Yeast suspension (1×10^7 cells/mL in Alsever's solution) was then added with a yeast-haemocyte ratio of 10:1 (Su et al., 2018). The yeast-haemocyte mixture was incubated at 25 °C for 30 min and then fixed with 100 μL of 2.5 % glutaraldehyde. Blood smears were subsequently prepared and stained with Wright's Gimesa stain (G1020, Solarbio, China). The phagocytic rate for each sample was analysed by the blood smear under an Olympus BX53 microscope (200 × magnification). The phagocytic activity of the haemocytes was estimated as the percentage of haemocytes that engulfed at least one yeast particle. At least 200 haemocytes were scored for each sample to ensure accuracy.

2.6. Determination of the haemocyte viability and caspase-3 activity

The haemocyte viability was assessed by a 3 - (4,5 - dimethylthiazol - 2 - yl) - 2,5 - diphenyl - tetrazolium bromide (MTT) reduction assay (Domart-Coulon et al., 2000) with commercial kits (C0009, Beyotime Biotechnology, China). Briefly, haemolymph was seeded into 96-well plates (100 μL/well) and mixed with 10 μL of MTT (5 mg/mL). After incubation at 37 °C for 4 h, 100 μL of formanzan lysis was added into each well. Subsequently, another incubation for 4 h was carried out. The optical density of each sample was then measured by using a microplate reader (Multiskan GO, Thermo, USA) at a wavelength of 570 nm. The haemocyte viability was subsequently calculated by comparing the obtained optical value to that of the control (Ong et al., 2017).

Following the manufacturer's instruction, the caspase-3 activity of the haemocytes was assessed with a colorimetric assay kit (C1115, Beyotime Biotechnology, China). After incubation of 50 μL of haemolymph with 50 μL of reaction buffer containing 10 μL caspase-3 substrate (Ac-DEVD-pNA, 2 nM) at 37 °C for 2 h, the absorbance value of each sample was determined at a wavelength of 405 nm using a microplate reader (Multiskan GO, Thermo, USA). The total protein concentration of each haemolymph sample was determined with a commercial kit (P0006C, Beyotime Biotechnology, China) using the Bradford method. The activity of caspase-3 was subsequently estimated as U_{casp} per mg protein, where U_{casp} is defined as the enzyme content cleaving 1 nmol of Ac-DEVD-pNA per hour at 37 °C. The same protein quantification method was also adopted for the estimation of the ATP content, PK activity, plasma cortisol concentration, and neurotransmitter content in this study.

2.7. Measurement of ROS content and the level of lipid peroxidation

The intracellular content of ROS in haemocytes was measured using a 2',7'-dichlorodihydrofluorescein-diacetate (DCFH-DA) ROS assay kit (S0033, Beyotime Biotechnology, China). According to the protocol provided with the kit, 50 μL of haemocytes was incubated in PBS containing 10 μM of DCFH-DA at 37 °C for 20 min. After washing with PBS for three times, the fluorescence intensity of each sample was determined with a microplate reader (Synergy Neo2, BioTek, USA) at the excitation and emission wavelengths of 488 and 525 nm, respectively. The relative intracellular content of ROS was then obtained by dividing the obtained fluorescence intensity by that of the control.

Lipid peroxidation in haemocytes was assessed by measuring the level of malondialdehyde (MDA), a terminal product of lipid peroxidation (Marnett, 1999). Following the provided instruction, the MDA concentration in the haemocytes was measured by thiobarbituric acid methods using a commercial kit (BC0025, Solarbio, China) with a microplate reader (Multiskan GO, Thermo, USA). After the determination

of the haemocyte concentrations using the method mentioned above, the MDA concentrations in the haemocytes were then standardised and expressed in nmol per 10^4 cells.

2.8. Measurements of ATP content and PK activity

The ATP content of the haemolymph was determined with an ATP assay kit (A095, Nanjing Jiancheng Bioengineering Institute, China) according to the manufacturer's instructions. Briefly, 30 μL of haemocytes was incubated with 300 μL of substrate solution and 30 μL of accelerant at 37 °C for 30 min. After mixing with 50 μL of precipitant, the mixture was centrifuged for 5 min at 5000 × g. Subsequently, 300 μL of the supernatant was mixed (1:1) with a chromogenic reagent, and then 500 μL of stop solution was added. The absorbance of each sample was determined at a wavelength of 636 nm using a microplate reader (Multiskan GO, Thermo, USA). The ATP content was then estimated with the obtained absorbance value and expressed as mmol per mg protein.

The activity of PK was determined with a commercial kit (A076, Nanjing Jiancheng Bioengineering Institute, China) according to the provided protocol. In brief, 20 μL of each haemocyte sample was mixed with 1.125 mL of PK assay buffer and then incubated at 37 °C for 15 min. The absorbance of each sample was measured immediately after the incubation with a spectrophotometer (UV-2100, Shanghai Jinghua Instruments, China) at a wavelength of 340 nm. The activity of PK was calculated as U_{PK} per mg protein, where U_{PK} is defined as the enzyme content causing the conversion of 1 μmol of substrate phosphoenolpyruvate into pyruvate per min at 37 °C.

2.9. Measurements of the plasma cortisol concentration

The haemolymph collected from each clam individual was immediately centrifuged (500 × g, 5 min, 4 °C). The obtained supernatant was used to measure the plasma cortisol concentration with commercial ELISA kits (ML003467, MLBIO Biotechnology, China) according to the provided instruction. First, 10 μL of the supernatant was mixed with 40 μL of the provided enzyme-labelled reagent and incubated at 37 °C for 1 h. Then 50 μL of chromogenic reagents A and B were sequentially added to the sample and incubated at 37 °C for 15 min before the addition of 50 μL of the terminator. The absorption of each sample was measured at a wavelength of 450 nm using a microplate reader (Multiskan GO, Thermo, USA). The concentration of cortisol was subsequently determined by referring the obtained absorption value to corresponding standard curves and expressed as ng cortisol per mg protein.

2.10. Quantification of the in vivo concentrations of ACh and GABA

Following the method of Guan et al. (2018), the concentrations of ACh and GABA in the haemolymph supernate were measured with ACh and GABA ELISA kits (ML095412 and ML086216, respectively, MLBIO Biotechnology, China). Briefly, 10 μL of each haemolymph supernate was seeded into 96-well plates containing 40 μL of diluent in each well and incubated at 37 °C for 1 h. After washing with wash buffer, the wells were incubated for another 15 min. After the addition of 50 μL of corresponding chromogenic reagent and stop solution, the absorptions were measured at a wavelength of 450 nm using a microplate reader (Multiskan GO, Thermo, USA). The concentrations of ACh and GABA in each sample were subsequently determined by comparing the obtained absorption values to the corresponding standard curves.

2.11. Analysis of the in vivo concentration of CYP1A1

The *in vivo* concentration of CYP1A1 in the digestive gland of *T. granosa* was determined with a CYP1A1 ELISA kit (ML063800, MLBIO Biotechnology, China). Briefly, frozen tissues were homogenised in

100 μL of PBS on ice with an electric homogeniser (ART, MICCRA D-1, Germany). After centrifugation at 1000 × g for 20 min (4 °C), the supernatant was collected and used for the measurement of CYP1A1. After 10 μL of the supernatant was mixed with 40 μL of the provided enzyme-labelled reagent, the mixture was incubated at 37 °C for 1 h. The sample was then mixed with chromogenic reagents A (50 μL) and B (50 μL), and incubated at 37 °C for 15 min before the addition of 50 μL of stop solution. The absorption of each sample was determined with a microplate reader (Multiskan GO, Thermo, USA) at the absorption wavelength of 450 nm. The concentration of CYP1A1 was subsequently determined by referring to the standard curves.

2.12. Transcriptome sequencing, analysis and validation

Total RNA from clams of the control and nanoscale MPs-, Ser-, and MP-Ser exposure groups were extracted with the EASY Spin Plus tissues/cells rapid RNA extraction kit (Aidlab, RN2802) according to the provided instruction. RNA contamination and integrity were assessed via electrophoresis (1 % agarose gels) and using an Agilent 2100 bioanalyzer (RNA Nano 6000 Assay Kit, Agilent Technologies, USA), respectively. The RNA purity was verified with a NanoDrop 1000 spectrophotometer (Thermo Scientific, USA). Sequencing libraries were generated using NEBNext Ultra RNA Library Prep Kit for Illumina (NEB, USA) following the manufacturer's protocols. The sequencing was performed by NovoGene Bioinformatics Technology Co. Ltd. (Beijing, China) on a HiSeq 2000 platform. The raw sequence reads were deposited in the Sequence Read Archive (SRA) at the National Centre for Biotechnology Information (NCBI) with an accession number of PRJNA598924. After trimming, the clean reads were mapped back to the reference genome using HISAT2 software (Version 2.0.5) and the gene expression levels were estimated by the fragment per kilo bases per million (PFKM). A differential expression analysis was performed using the DESeq2 R package (Version 1.16.1). To control the false discovery rate, the original *p* values were adjusted by the Benjamini-Hochberg false discovery rate and only genes with an adjusted *p* value (adj-*p*) < 0.05 and $|\log_2 (\text{fold change})| > 0$ were assigned as differentially expressed unigenes (DEGs). The DEGs were subjected to Gene ontology (GO) enrichment and Kyoto Encyclopedia of Genes and Genomes (KEGG) pathway analyses (Ashburner et al., 2000; Altermann & Klaenhammer, 2005).

The real-time quantitative polymerase chain reaction (qPCR) analysis was performed to validate nine representative DEGs with the same RNA samples for transcriptome sequencing. The real-time qPCR was conducted on the StepOnePlus Real-Time PCR System (Applied Biosystems, USA) in triplicates following the method of previous studies (Shi et al., 2017, 2019). The expression of genes was calculated as the relative expression to 18 s rRNA using the $2^{-\Delta\Delta Ct}$ method (Livak and Schmittgen, 2001). The primers used are listed in Table S1. All primers were synthesised by TsingKe Biotech (Beijing, China).

2.13. Statistical analysis

A one-way analysis of variance (ANOVA) followed by Tukey's post hoc tests were conducted to compare the haemocyte counts, phagocytic activities, cell viabilities, ROS contents, MDA levels, ATP contents, enzyme activities (caspase-3 and PK) as well as the *in vivo* concentrations of cortisol, ACh, GABA, and CYP1A1 among the experimental groups. Duncan's multiple range tests were conducted to compare the expression levels of the tested genes among the different experimental groups. In all analyses, the Levene's test and Shapiro-Wilk's test were used to verify the homogeneity and normality of variances, respectively. All analyses were performed with statistical software OriginPro 8.0. A *p* or adj-*p* value less than 0.05 was adopted as statistical significance.

3. Results

3.1. Impacts of the exposure to the MPs, Ser and their combination on the total count and phagocytosis of haemocytes

Compared to those of control, significant reductions in THC ($F_{5,48}$ = 62.10, $p < 0.05$) and phagocytosis ($F_{5,48}$ = 215.66, $p < 0.05$) of haemocytes were observed in the clams exposed to the MPs, Ser, and MP-Ser (Table 1). Though no significant differences in the THC and phagocytosis were detected between the nanoscale- (500 nm) and microscale- (30 μm) MP-exposure groups (Table 1, $p > 0.05$), evident size-dependent interactions of the MPs with Ser were demonstrated. The toxicity of Ser was not affected by the copresence of microscale MPs. However, coexposure to Ser and nanoscale MPs resulted in an aggravated immunotoxicity indicated by the significantly reduced THC and phagocytosis, which were approximately 51.36 % and 74.74 % of those of the group exposed to only Ser (Table 1), respectively.

3.2. Impacts of the exposure to the MPs, Ser and their combination on the haemocyte viability and caspase-3 activity

Exposure to the MPs, Ser, and their combination all led to significant reductions in haemocyte viability in *T. granosa* (Fig. 1A, $F_{5,48}$ = 23.87, $p < 0.05$). Although the haemocyte viability was not significantly suppressed by microscale MPs ($p < 0.05$), nanoscale MPs showed a significant toxicity to the viability of haemocyte ($p < 0.05$). Coexposure to Ser and nanoscale MPs resulted in enhanced toxic effect on the haemocyte viability than that of the exposure to only MPs (Fig. 1A, $p < 0.05$), while no statistically significant difference was observed between the microscale MPs exposure groups and corresponding Ser-MPs coexposure groups (Fig. 1A, $p > 0.05$).

Compared to that of the control, exposure to MPs, Ser and their combination increased the caspase-3 activities in the haemocytes (Fig. 1B, $F_{5,48}$ = 412.79, $p < 0.05$), which indicates increased apoptosis rates upon these treatments. Moreover, compared to that of the Ser exposure group, coexposure with MPs at both nanoscale and microscale led to significant increases (approximately 1.27 and 1.14 times, respectively) in caspase-3 activity of the haemocytes ($p < 0.05$), which suggests a synergetic effect of the MPs and Ser on the apoptosis of haemocytes.

3.3. Impacts of the exposure to the MPs, Ser and their combination on the intracellular contents of ROS and MDA in the haemocytes

Intracellular ROS content in haemocytes, indicated by the specific fluorescent intensities, were significantly induced by MPs, Ser, and their combination (Fig. 2A, $F_{5,48}$ = 140.40, $p < 0.05$). Furthermore, coexposure with microscale or nanoscale MPs significantly increased the intracellular ROS content in haemocytes, which was approximately 1.52 and 1.69 times those obtained upon the exposure to Ser, respectively. Significant differences in intracellular ROS content were also detected between the MPs exposure and corresponding Ser-MPs coexposure groups ($p < 0.05$).

Though the MDA level in the haemocytes was not affected by the exposure to Ser (Fig. 2B, $p > 0.05$), the exposure to MPs and Ser-MPs led to significant increases in MDA content (Fig. 2B, $F_{5,48}$ = 85.53, $p < 0.05$). In addition, compared to those obtained upon the exposure to Ser and MPs, clams coexposed to Ser and MPs had significantly higher MDA content ($p < 0.05$). For example, the MDA contents in the haemocytes after the coexposure to nanoscale MPs and Ser was increased by approximately 177.07 % and 74.75 % of those exposed Ser and nanoscale MPs, respectively.

3.4. Impacts of the exposure to the MPs, Ser and their combination on the ATP content and activity of PK in the haemocytes

Compared to that of the control, the exposure to the nanoscale MPs led to a significant reduction in ATP content in the haemocytes (Fig. 3A, $F_{5,48}$ = 9.61, $p < 0.05$). Though the ATP content in the haemocytes was not affected by the Ser treatment, coexposure of clams to Ser and nanoscale MPs resulted in a significant reduction in ATP content compared to those for the separate treatments ($p < 0.05$), which indicates a synergetic effect of the nanoscale MPs and Ser on the ATP content. For example, the haemocyte ATP content of the clams coexposed to Ser and nano-sclae MPs was only approximately 85.12 % and 62.70 % of those of the Ser- and MPs- (500 nm) single exposure groups, respectively. The activity of PK was significantly suppressed by the MPs and Ser exposure (Fig. 3B, $F_{5,48}$ = 39.40, $p < 0.05$). Moreover, compared to corresponding single treatment groups, the coexposure of clams to Ser and nanoscale MPs caused further decreases in PK activity ($p < 0.05$), which was only approximately 76.2 % and 89.8 % of those of the Ser and MPs (500 nm) single exposure groups, respectively.

3.5. Impacts of exposure to MPs, Ser and their combination on the concentration of plasma cortisol

Compared to that of the control, the Ser exposure led to a significant increase in plasma cortisol concentration (Fig. 4, $F_{5,30}$ = 164.17, $p < 0.05$). In addition, though the plasma cortisol concentration was not affected by exposure to MPs alone, coexposure of clams to Ser and nanscale MPs resulted in a significant increase in plasma cortisol concentration, which was 1.1 times higher than that of the Ser single treatment group.

3.6. Impacts of exposure to MPs, Ser and their combination on the in vivo concentrations of ACh and GABA

The *in vivo* concentrations of both ACh (Fig. 5A, $F_{5,48}$ = 39.59, $p < 0.05$) and GABA (Fig. 5B, $F_{5,48}$ = 90.62, $p < 0.05$) were significantly increased by the Ser exposure by approximately 16.1 % (ACh) and 19.1 % (GABA) of those of the control, respectively. Moreover, compared to those for the separate treatments with Ser and MPs, coexposure of clams to Ser and MPs led to significantly higher concentrations of *in vivo* ACh and GABA ($p < 0.05$), which indicated a synergetic effect of Ser and MPs.

3.7. Impacts of exposure to the MPs, Ser and their combination on the in vivo concentration of CYP1A1

Compared to that of the control, the *in vivo* concentrations of CYP1A1 were significantly reduced by exposure to MPs and Ser-MPs, whereas the Ser exposure led to a significant increase in *in vivo* concentration of CYP1A1 (Fig. 6, $F_{5,48}$ = 21.48, $p < 0.05$). Furthermore, compared to the corresponding Ser and MPs single exposure groups, coexposure of clams to Ser and nanoscale MPs resulted in significant further decreases in CYP1A1 content (reduced by approximately 11.5 %

Table 1

Total counts (THC) and phagocytosis of haemocytes of *T. granosa* after 14 days exposure to MPs, Ser, and their combination. Different uppercase letters indicate significant differences ($p < 0.05$) in the same column.

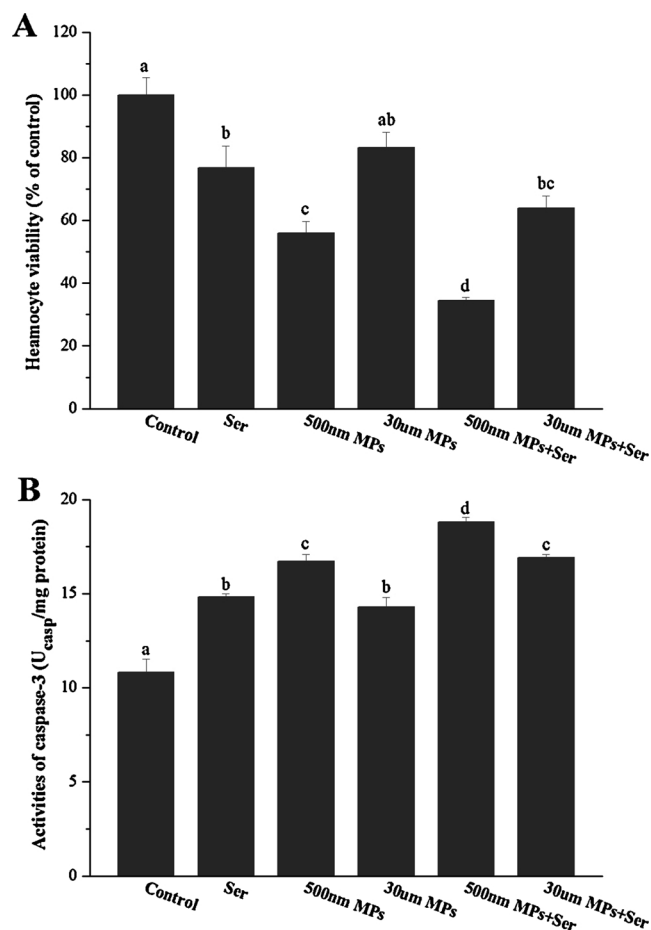| Group	THC ($\times 10^8$ cell/mL)	Phagocytosis (%)
Control	2.41 ± 0.33[a]	33.80 ± 1.32[a]
Ser	1.55 ± 0.12[b]	25.40 ± 0.71[b]
500 nm MPs	1.68 ± 0.18[b]	22.79 ± 0.35[b]
30 μm MPs	1.98 ± 0.16[c]	23.94 ± 0.61[b]
500 nm MPs + Ser	0.80 ± 0.18[d]	18.99 ± 0.74[c]
30 μm MPs + Ser	1.48 ± 0.19[b]	25.32 ± 0.99[b]

A

B

Fig. 1. Haemocyte viabilities (A) and caspase-3 activities (B) of *T. granosa* after 14 days of exposure to MPs, Ser, and their combination. Mean values that do not share the same superscript were significantly different ($p < 0.05$)
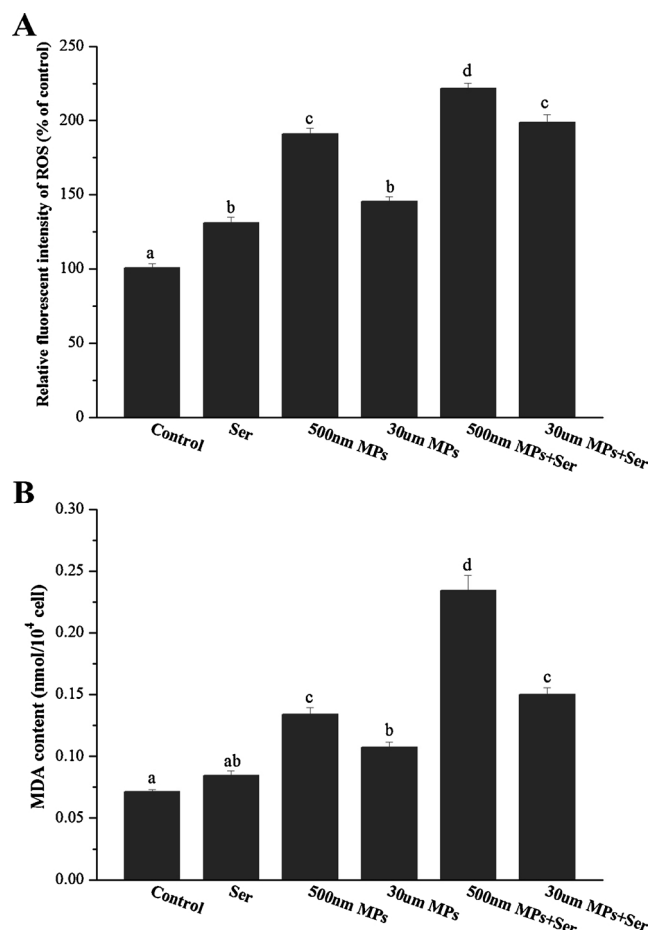
A

B

Fig. 2. Fluorescence intensities of intracellular ROS (A) and MDA content (B) in the haemocytes of *T. granosa* after 14 days of exposure to MPs, Ser and their combination. Mean values that do not share the same superscript were significantly different ($p < 0.05$).

and 7.0 %, respectively, $p < 0.05$).

3.8. Impacts of exposure to MPs, Ser and their combination on the transcriptome of T. granosa

The Illumina sequencing yielded approximately 60 million reads per sample (Table S2). After discarding the reads with adapters, poly-N > 10 %, and any possible contaminants, in total, 532.12 million clean reads were obtained. The clean reads were mapped to the genome of *T. granosa*. A summary of raw and clean reads is presented as a supplementary material (Table S2). The sequencing was validated by results of real-time qPCR, which show an evident correlation of the fold change in expression with the RNA sequencing results (Fig. S1). The heatmap and hierarchical clustering performed with DEGs revealed substantial differences between the different experimental groups (Fig. 7A). In total, 1958 and 2904 gene transcripts were differentially expressed in the coexposure group relative to those separately treated with Ser and MPs, respectively (Fig. 7).

The GO analysis revealed that a total of 103 (85 up-regulated and 18 down-regulated) GO terms were significantly (adj-$p < 0.05$) enriched in the coexposure group in comparison to the Ser exposure group (Table 2). The down-regulated DEGs detected were those involved in "DNA replication initiation" (GO:0006270), "immune response" (GO:0006955), and "immune system process" (GO:0002376). Compared to the MPs exposure group, 159 (115 up-regulated and 44 down-regulated) GO terms were significantly (adj-$p < 0.05$) enriched in coexposure group (Table 2). The down-regulated DEGs detected were those involved in "DNA replication initiation", "immune response", and

"response to stress" (GO:0006950). Compared to those of Ser and nanoscale MPs single exposure groups, most of the significantly up-regulated DEGs detected in the coexposure group were those closely related to the lipid metabolism processes, such as the "fatty acid metabolic process" (GO:0006631), "lipid metabolic process" (GO:0006629), and "response to lipid" (GO:0033993) (Table 2). The KEGG enrichment analyses showed that eight pathways were significantly enriched in the coexposure group in comparison to the Ser and nanoscale MPs single exposure groups (Fig. 8), including "peroxisome" (spu04146), "lysosome" (spu04142), "phagosome" (spu04145) and "fatty acid metabolism" (spu01212).

4. Discussion

Though coexposure to pharmaceuticals and MPs may frequently occur in estuaries and coastal areas (Graca et al., 2017; Li et al., 2019; Tang et al., 2020), their combined impacts on marine benthic organisms are still poorly understood to date. Results obtained in this study showed that both Ser and MPs (diameter 500 nm and 30 μm) can significantly suppress the immune responses of *T. granosa*, which may be attributed to a series of physiological and molecular alterations. In addition, an evident synergistic immune-toxic effect of Ser and nanoscale MPs was observed, indicating the size-dependent interaction between Ser and MPs. This suggests that the coexposure to Ser and smaller size MPs may pose more severe threats to bivalve species than those upon the exposure to Ser and coexposure to Ser and larger MPs.

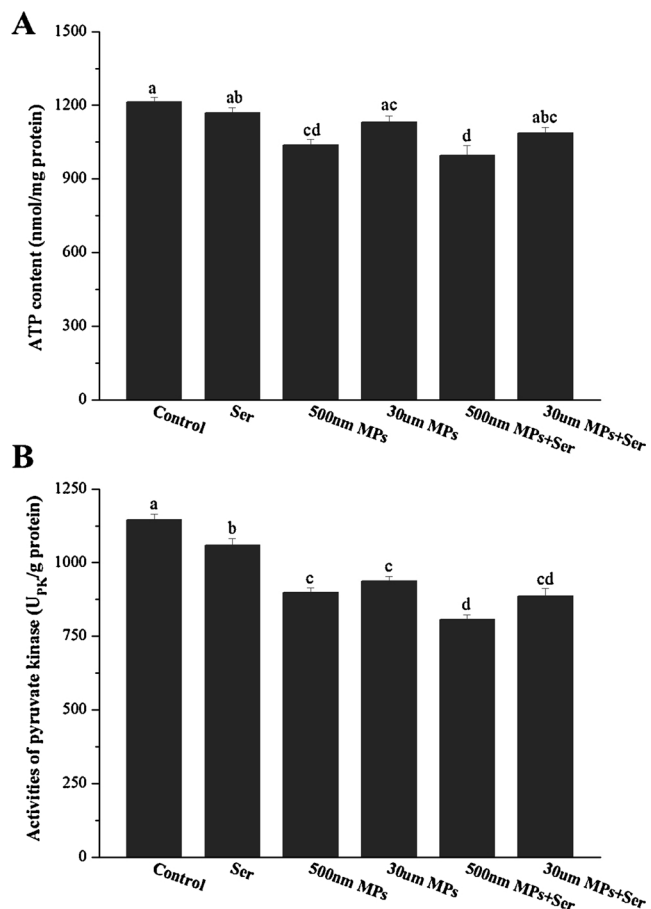Considering the lack of antigen-antibody-mediated immune

Fig. 3. ATP contents (A) and pyruvate kinase (PK) activities (B) in the haemocytes of *T. granosa* after 14 days of exposure to MPs, Ser, and their combination. Mean values that do not share the same superscript were significantly different ($p < 0.05$).

Fig. 5. The *in vivo* concentrations of (A) ACh and (B) GABA in *T. granosa* after 14 days of exposure to MPs, Ser, and their combination. Mean values that do not share the same superscript were significantly different ($p < 0.05$).

Fig. 4. The *in vivo* concentrations of plasma cortisol of *T. granosa* after 14 days of exposure to MPs, Ser, and their combination. Mean values that do not share the same superscript were significantly different ($p < 0.05$).
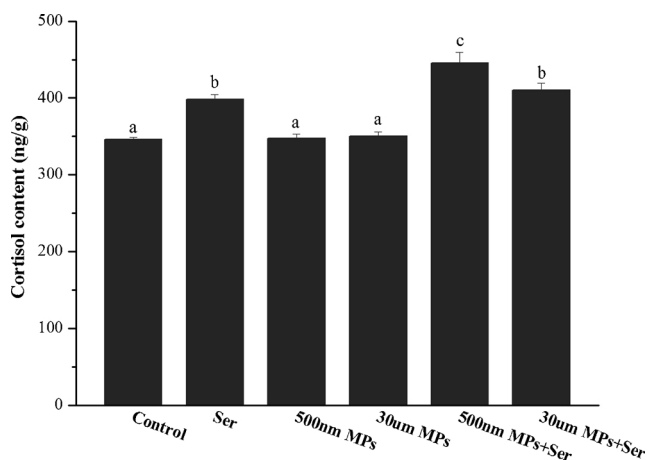

Fig. 6. The *in vivo* concentrations of CYP1A1 in the digestive gland of *T. granosa* after 14 days of exposure to MPs, Ser, and their combination. Mean values that do not share the same superscript were significantly different ($p < 0.05$).

responses, the haemocytes are regarded as the main immune cells of marine bivalves to remove invaded exogenous particles such as pathogens through the process of phagocytosis (Loker et al., 2004). In the present study, evident immunotoxicities indicated by the reductions in total count and phagocytic activity of haemocytes were detected for both Ser and MPs. The reductions in haemocyte count upon the Ser and MPs exposure may be attributed to the induction of oxidative damage
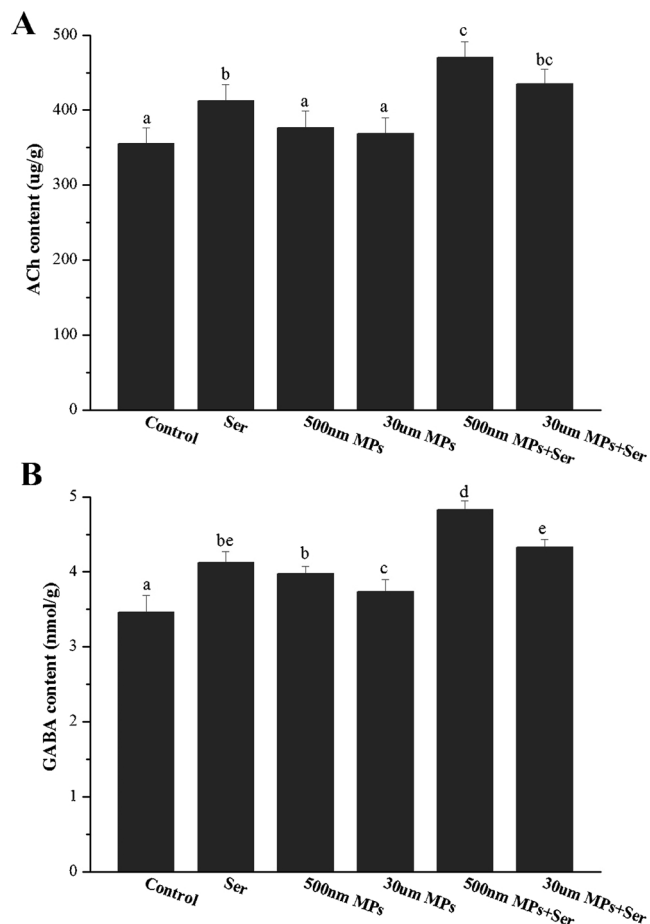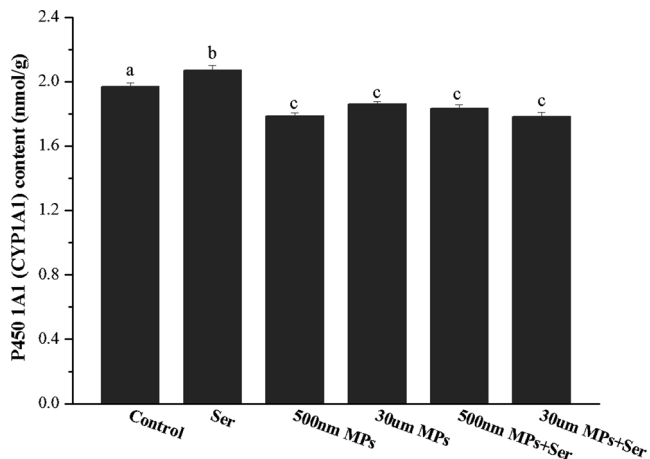
on haemocytes. It is generally accepted that the generation of intracellular ROS and lipid peroxidation (MDA) could trigger apoptosis of a variety of cells including haemocytes (Premanathan et al., 2011). Thus the increases in intracellular ROS and MDA levels upon Ser and MPs exposure could induce the apoptosis of haemocytes and lead to reductions in THC. This inference was further confirmed by the
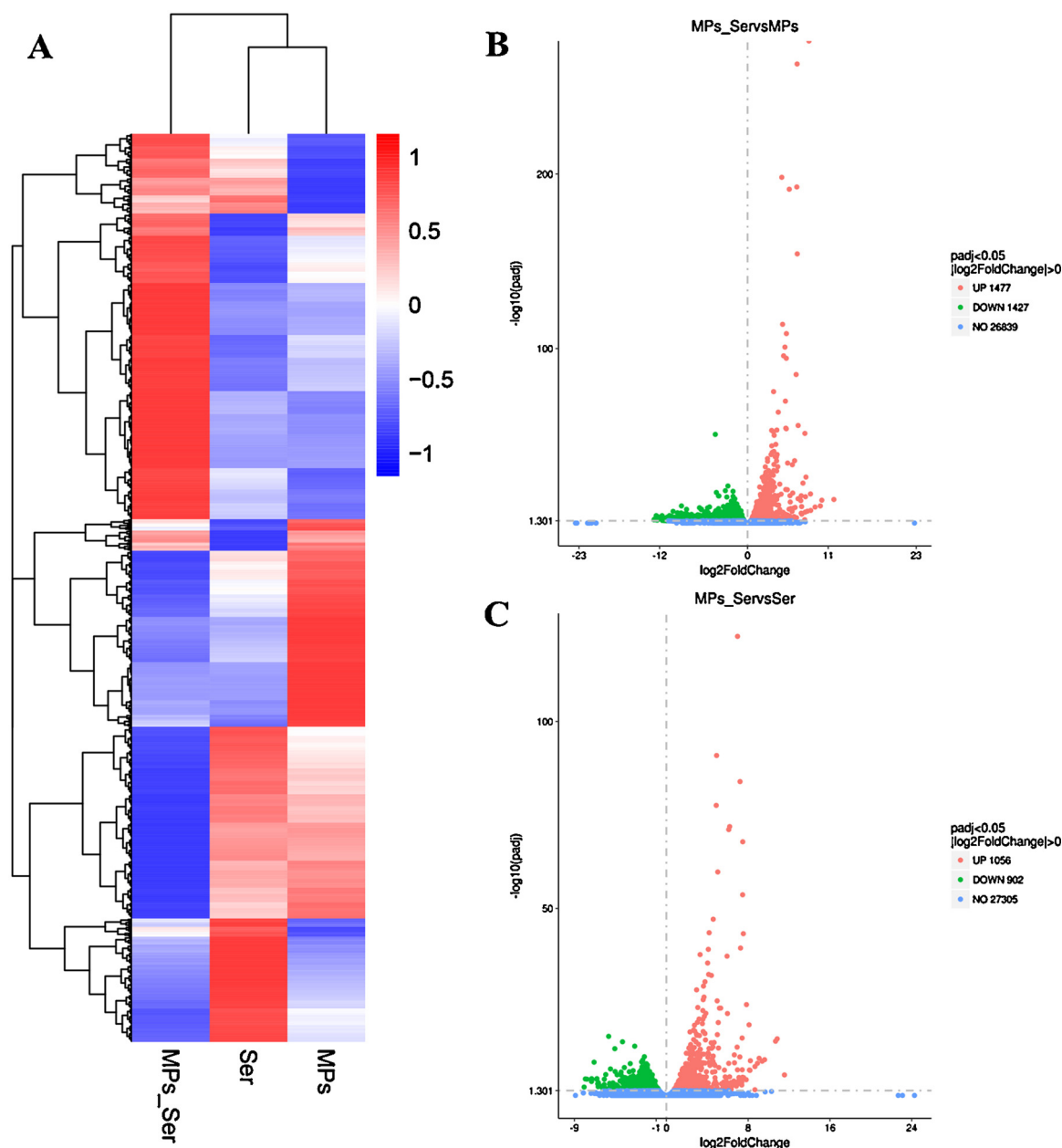
Fig. 7. Hierarchical cluster (A) of differentially expressed unigenes (DEGs) across treatments and volcano plots of DEGs of the coexposure group versus those exposed to nanoscale MPs (B) and Ser (C) alone. Genes and samples are clustered by similarity of expression (Left and top, respectively). DEGs were selected by adjusted p value < 0.05 and |$\log_2$ (fold change)| > 0.

induction of caspase-3 upon Ser and MPs exposure observed in this study. According to the data obtained, Ser and MPs may constrain the phagocytic activity of haemocytes through the following physiological and molecular impacts.

First, the phagocytosis is an energy-consuming process (Turvey & Broide, 2010). However, significant reductions in ATP content and PK activity in haemocytes were observed after MP exposure in this study. Thus, the MPs may inhibit the phagocytic activity of the haemocytes by constraining the energy (ATP content) available for phagocytosis. According to previous studies, the reduction in energy availability can be attributed to the blockage of the intestine, reduction in feeding, and arrested energy assimilation upon MPs exposure (Barnes et al., 2009; Yin et al., 2018). Furthermore, it has been suggested that organisms would alter energetic trade-offs between different physiological and behavioural processes to meet the increased energetic demands under the challenge of environmental stressors, such as climate change, food

shortage, and pollutants (Delaporte et al., 2006; Mogensen & Post, 2012; Roberts et al., 2013). For example, more energy of the oyster *Crassostrea gigas* would be allocated to gonad development rather than haemocyte activities such as phagocytosis under food shortage (Delaporte et al., 2006). In this respect, the physiological stress induced by MPs or Ser, as indicated by the increase in plasma cortisol level detected (Eames et al., 2010), may also lead to a reduction in the energy budget for phagocytosis.

Second, MPs and Ser may affect the phagocytosis of haemocytes through disturbing the neuroendocrine system as well. Classical hormones and neurotransmitters released by the neuroendocrine system, such as cortisol, ACh, and GABA, can mediate a vast array of immunomodulatory processes in both vertebrates and marine molluscs (Li et al., 2016; Liu et al., 2017; Guan et al., 2018). For instance, the haemocyte phagocytosis of oyster *C. gigas* induced by lipopolysaccharide (LPS) could be suppressed by the addition of GABA (Li et al.,
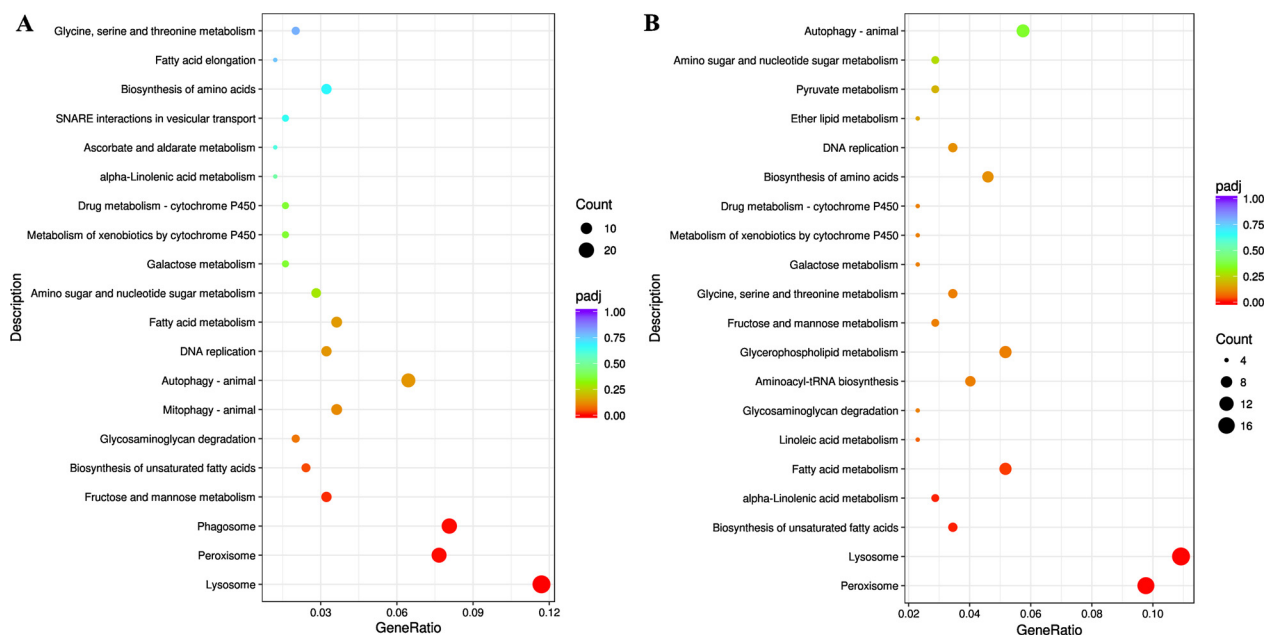
Table 2

Gene ontology (GO) enrichment analysis of differentially expressed unigenes (DEGs) of the coexposed group versus those exposed to MPs and Ser.

MPs_ServsMPs group: coexposure group versus nanoscale MPs exposure group, MPs_ServsSer MPs_group: coexposure group versus Ser exposure group, BP: biological process, CC: cellular component, MF: molecular function, down or up: terms enriched in the set of down- or up-regulated DEGs, respectively, count: count of DEGs, adj-*p*: adjusted *p* value. The DEGs were selected by adj-*p* value < 0.05 and |log$_2$ (fold change)| > 0.

Group	Regulation	Category	GO ID	GO term	Count	Adj-*p*
MPs_ServsMPs	Down	BP	GO:0006979	response to oxidative stress	13	2.11E-05
			GO:0005975	carbohydrate metabolic process	29	9.93E-04
			GO:0002376	immune system process	8	1.01E-03
			GO:0006955	immune response	8	1.01E-03
			GO:0006270	DNA replication initiation	5	3.76E-03
			GO:0006261	DNA-dependent DNA replication	6	3.96E-03
			GO:0006950	response to stress	21	9.23E-03
		CC	GO:0005576	extracellular region	30	7.62E-08
			GO:0005615	extracellular space	7	2.53E-04
			GO:0044421	extracellular region part	9	3.20E-04
		MF	GO:0004601	peroxidase activity	15	3.26E-07
			GO:0005044	scavenger receptor activity	15	8.68E-07
			GO:0016209	antioxidant activity	15	9.03E-07
			GO:0005164	tumor necrosis factor receptor binding	7	4.67E-05
			GO:0030234	enzyme regulator activity	20	3.23E-04
	UP	BP	GO:0006631	fatty acid metabolic process	12	6.06E-06
			GO:0019752	carboxylic acid metabolic process	26	2.73E-05
			GO:0006082	organic acid metabolic process	26	2.86E-05
			GO:0006629	lipid metabolic process	31	3.99E-05
			GO:0033993	response to lipid	13	2.74E-04
			GO:0071396	cellular response to lipid	13	2.74E-04
			GO:0009725	response to hormone	13	2.24E-05
		CC	GO:0012506	vesicle membrane	7	1.34E-05
			GO:0030120	vesicle coat	7	1.34E-05
			GO:0031410	cytoplasmic vesicle	7	2.88E-05
			GO:0005777	peroxisome	5	3.86E-04
		MF	GO:0020037	heme binding	33	1.77E-06
			GO:0046906	tetrapyrrole binding	33	1.86E-06
			GO:0016874	ligase activity	16	4.00E-04
			GO:0016887	ATPase activity	17	6.07E-04
MPs_ServsSer	Down	BP	GO:0006270	DNA replication initiation	5	2.06E-04
			GO:0009888	tissue development	5	2.97E-04
			GO:0002376	immune system process	6	7.86E-04
			GO:0006955	immune response	6	7.86E-04
			GO:0006260	DNA replication	7	7.51E-03
		MF	GO:0005126	cytokine receptor binding	6	4.11E-05
			GO:0005164	tumor necrosis factor receptor binding	6	4.11E-05
			GO:0032813	tumor necrosis factor receptor superfamily binding	6	4.11E-05
			GO:0030246	carbohydrate binding	9	8.31E-03
	UP	BP	GO:0006631	fatty acid metabolic process	12	5.87E-07
			GO:0019752	carboxylic acid metabolic process	25	2.41E-06
			GO:0006082	organic acid metabolic process	25	2.54E-06
			GO:0006629	lipid metabolic process	27	2.43E-05
			GO:0044281	small molecule metabolic process	31	9.29E-04
			GO:0044255	cellular lipid metabolic process	17	9.29E-04
			GO:0033993	response to lipid	11	9.29E-04
			GO:0071396	cellular response to lipid	11	9.29E-04
			GO:0016042	lipid catabolic process	9	9.29E-04
		CC	GO:0005777	peroxisome	7	9.23E-05
			GO:0042579	microbody	7	9.23E-05
		MF	GO:0016705	oxidoreductase activity, acting on paired donors, with incorporation or reduction of molecular oxygen	38	2.88E-13
			GO:0020037	heme binding	31	1.44E-07
			GO:0004497	monooxygenase activity	11	5.55E-05
			GO:0016887	ATPase activity	21	1.57E-07
			GO:0003997	acyl-CoA oxidase activity	5	3.36E-04
			GO:0001071	nucleic acid binding transcription factor activity	6	6.73E-04
			GO:0015171	amino acid transmembrane transporter activity	4	3.70E-02

2016). Similarly, a recent study demonstrated that cortisol (15 and 30 ng/mL) can effectively inhibit the NFκB signalling pathway, a key regulatory molecular pathway for immune activities including phagocytosis (Dong et al., 2018). Therefore, the significant alterations in the *in vivo* contents of hormones and neurotransmitters (cortisol, ACh, and GABA) upon MPs and Ser exposure detected in this study may also hamper the phagocytosis of haemocytes through their modulating effects.

An evident synergistic immune-toxic effect of Ser and MPs was observed in this study, which may be caused by following factors. As both Ser and MPs are immuno-toxic to *T. granosa*, the synergetic effect observed may be simply due to the addition of the immuno-toxic impacts of these two types of pollutants. Notably, the GO enrichment analyses revealed that compared to those treated with Ser or MPs, many genes in "immune response" and "DNA replication initiation" were significantly down-regulated upon Ser-MPs coexposure. Considering their important roles in immune response and cell proliferation, the down-regulation of these genes may hamper the immune activity and recruitment of haemocytes, which may therefore result in an aggravated immune-toxicity. Furthermore, it has been suggested that the

Fig. 8. KEGG analysis of differentially expressed unigenes (DEGs) of the coexposure group versus those exposed to nanoscale MPs (A) and Ser (B) alone. DEGs were selected by adjusted *p* value < 0.05 and |log$_2$ (fold change)| > 0.

dysregulation of lipid metabolism can impair innate immune responses (Im et al., 2011; Han et al., 2018). Results obtained in this study showed that coexposure to Ser and MPs led to alterations in lipid metabolism processes such as the fatty acid metabolic process and lipid metabolic process, therefore the aggravated toxic impacts may be caused by alterations in these processes upon Ser-MPs coexposure. Similarly, compared to those exposed to Ser or MPs, the KEGG analysis revealed that the DEGs detected in the coexposure group were mainly from "peroxisome", "lysosome" and "phagosome" pathways. Since these pathways are important in the regulation of ROS and phagocytosis, alterations in these key pathways may also lead to aggravated toxicity (Repnik et al., 2012; Dupré-Crochet et al., 2013).

Furthermore, the detected synergetic effect may also originate from the interaction between Ser and MPs. Considering the relatively high specific surface area and penetration capability, the presence of MPs may facilitate the internalisation of Ser by marine organisms through the "Trojan horse" effect, which could subsequently lead to aggravated toxicity (Rochman et al., 2014; Brennecke et al., 2016). In addition, it has been suggested that MPs can reach the vicinity of the endoplasmic reticulum and inhibit the enzymatic activity of P450 isoenzymes, key enzymes involved in the drug/toxicant metabolism (Nash et al., 2014). Since the concentration of the important drug-metabolising cytochrome P450 isoenzyme CYP1A1 (Sarasquete & Segner, 2000; Nash et al., 2014) was significantly reduced upon the MPs exposure, the coexposure to Ser and MPs could result in aggravated toxicity due to the hampered detoxification, which fails to exclude Ser out of the body.

Notably, the evident synergistic immune-toxic effect was observed only for Ser and nanoscale MPs, which may be due to the size-dependent interactions between Ser and MPs. Nanoscale MPs have a considerably larger specific surface area than that of microscale MPs, which could carry higher amount of pollutants into the organisms and thus result in higher toxicity. Van Cauwenberghe and Janssen (2014) reported that the majority of larger MPs (diameter > 25 μm) can be removed from the bodies of *M. edulis* and *C. gigas* after a depuration period of three days, while the smaller MPs were still retained in the tissues and circulatory system. As a result, compared to the larger MPs (30 μm), the smaller nanoscale MPs (500 nm) tested in this study would retain longer in clams and consequently have more time to discharge the carried Ser. Furthermore, due to their small sizes, the nanoscale

MPs may enter the cell easier than the larger MPs and thus exhibit a stronger inhibition on CYP isoenzymes (Fröhlich et al., 2010), which could hamper the exclusion of Ser and subsequently result in higher toxicity as well.

In summary, for the first time, the present study demonstrates that the presence of MPs increased the immunotoxicity of Ser to marine organisms. The nanoscale MPs alone or in combination with other toxicants could exert more toxic effects on marine organisms than those by the larger MPs. Considering these results, further studies on the combined effects of other pollutants and MPs particularly at the nanoscale are of interest.

CRediT authorship contribution statement

Wei Shi: Conceptualization, Investigation, Methodology, Writing - original draft, Writing - review & editing. **Yu Han:** Software, Data curation, Validation, Investigation. **Shuge Sun:** Visualization, Investigation. **Yu Tang:** Resources, Investigation. **Weishang Zhou:** Formal analysis, Investigation. **Xueying Du:** Visualization, Data curation. **Guangxu Liu:** Conceptualization, Project administration, Supervision, Funding acquisition.

Declaration of Competing Interest

The authors declare that they have no known competing financial interests or personal relationships that could have appeared to influence the work reported in this paper.

Appendix A. Supplementary data

Supplementary material related to this article can be found, in the online version, at doi:https://doi.org/10.1016/j.jhazmat.2020.122603.

References

Altermann, E., Klaenhammer, T.R., 2005. PathwayVoyager: pathway mapping using the Kyoto Encyclopedia of Genes and Genomes (KEGG) database. BMC Genomics 6, 60.

Andrady, A.L., 2011. Microplastics in the marine environment. Mar. Pollut. Bull. 62, 1596–1605.

Ashburner, M., Ball, C.A., Blake, J.A., Botstein, D., Butler, H., Cherry, J.M., Davis, A.P., Dolinski, K., Dwight, S.S., Eppig, J.T., 2000. Gene ontology: tool for the unification of biology. Nat. Genet. 25, 25–29.

Avio, C.G., Gorbi, S., Milan, M., Benedetti, M., Fattorini, D., d'Errico, G., Pauletto, M., Bargelloni, L., Regoli, F., 2015. Pollutants bioavailability and toxicological risk from microplastics to marine mussels. Environ. Pollut. 198, 211–222.

Barnes, D.K., Galgani, F., Thompson, R.C., Barlaz, M., 2009. Accumulation and fragmentation of plastic debris in global environments. Philos. T. R. Soc. B 364, 1985–1998.

Besseling, E., Wang, B., Lürling, M., Koelmans, A.A., 2014. Nanoplastic affects growth of *S. obliquus* and reproduction of *D. magna*. Environ. Sci. Technol. 48, 12336–12343.

Brennecke, D., Duarte, B., Paiva, F., Caçador, I., Canning-Clode, J., 2016. Microplastics as vector for heavy metal contamination from the marine environment. Estuar. Coast. Shelf S. 178, 189–195.

Browne, M.A., Crump, P., Niven, S.J., Teuten, E., Tonkin, A., Galloway, T., Thompson, R., 2011. Accumulation of microplastic on shorelines worldwide: sources and sinks. Environ. Sci. Technol. 45, 9175–9179.

Canesi, L., Lorusso, L., Ciacci, C., Betti, M., Regoli, F., Poiana, G., Gallo, G., Marcomini, A., 2007. Effects of blood lipid lowering pharmaceuticals (bezafibrate and gemfibrozil) on immune and digestive gland functions of the bivalve mollusc, *Mytilus galloprovincialis*. Chemosphere 69, 994–1002.

Chen, Q., Gundlach, M., Yang, S., Jiang, J., Velki, M., Yin, D., Hollert, H., 2017. Quantitative investigation of the mechanisms of microplastics and nanoplastics toward zebrafish larvae locomotor activeity. Sci. Total Environ. 584–585, 1022–1031.

Christen, V., Hickmann, S., Rechenberg, B., Fent, K., 2010. Highly active human pharmaceuticals in aquatic systems: a concept for their identification based on their mode of action. Aquat. Toxicol. 96, 167–181.

Delaporte, M., Soudant, P., Lambert, C., Moal, J., Pouvreau, S., Samain, J.F., 2006. Impact of food availability on energy storage and defense related hemocyte parameters of the Pacific oyster *Crassostrea gigas* during an experimental reproductive cycle. Aquaculture 254, 571–582.

Détrée, C., Gallardo-Escárate, C., 2018. Single and repetitive microplastics exposures induce immune system modulation and homeostasis alteration in the edible mussel *Mytilus galloprovincialis*. Fish Shellfish Immun. 83, 52–60.

Domart-Coulon, I., Auzoux-Bordenave, S., Doumenc, D., Khalanski, M., 2000. Cytotoxicity assessment of antibiofouling compounds and by-products in marine bivalve cell cultures. Toxicol. in Vitro 14, 245–251.

Dong, J., Qu, Y., Li, J., Cui, L., Wang, Y., Lin, J., Wang, H., 2018. Cortisol inhibits NF-κB and MAPK pathways in LPS activated bovine endometrial epithelial cells. Int. Immunopharmacol. 56, 71–77.

Dupré-Crochet, S., Erard, M., Nüße, O., 2013. ROS production in phagocytes: why, when, and where? J. Leukocyte Biol. 94, 657–670.

Eames, S.C., Philipson, L.H., Prince, V.E., Kinkel, M.D., 2010. Blood sugar measurement in zebrafish reveals dynamics of glucose homeostasis. Zebrafish 7, 205–213.

Franzellitti, S., Buratti, S., Capolupo, M., Du, B., Haddad, S.P., Chambliss, C.K., Brooks, B.W., Fabbri, E., 2014. An exploratory investigation of various modes of action and potential adverse outcomes of fluoxetine in marine mussels. Aquat. Toxicol. 151, 14–26.

Fröhlich, E., Kuznik, T., Samberger, C., Roblegg, E., Wrighton, C., Pieber, T.R., 2010. Size-dependent effects of nanoparticles on the activity of cytochrome P450 isoenzymes. Toxicol. Appl. Pharm. 242, 326–332.

Furlong, E.T., Kinney, C.A., Ferrer, I., 2004. Pharmaceuticals and personal-care products in solids: analysis and field results for sediment, soil, and biosolid samples. In: Proceedings, 228th American Chemical Society National Meeting. Philadelphia, PA, USA, August 22–26.

Goldstein, M.C., Rosenberg, M., Cheng, L., 2012. Increased oceanic microplastic debris enhances oviposition in an endemic pelagic insect. Biol. Letters 8, 817–820.

Graca, B., Szewc, K., Zakrzewska, D., Dołega, A., Szczerbowska-Boruchowska, M., 2017. Sources and fate of microplastics in marine and beach sediments of the Southern Baltic Sea - a preliminary study. Environ. Sci. Pollut. R. 24, 7650–7661.

Guan, X., Shi, W., Zha, S., Rong, J., Su, W., Liu, G., 2018. Neurotoxic impact of acute TiO$_2$ nanoparticle exposure on a benthic marine bivalve mollusk, *Tegillarca granosa*. Aquat. Toxicol. 200, 241–246.

Guan, X., Tang, Y., Zha, S., Han, Y., Shi, W., Ren, P., Yan, M., Pan, Q., Hu, Y., Fang, J., 2019. Exogenous Ca^{2+} mitigates the toxic effects of TiO$_2$ nanoparticles on phagocytosis, cell viability, and apoptosis in haemocytes of a marine bivalve mollusk, *Tegillarca granosa*. Environ. Pollut. 252, 1764–1771.

Han, Y., Shi, W., Rong, J., Zha, S., Guan, X., Sun, H., Liu, G., 2019. Exposure to waterborne nTiO$_2$ reduces fertilization success and increases polyspermy in a bivalve mollusc: a threat to population recruitment. Environ. Sci. Technol. 53, 12754–12763.

Han, Y., Lin, C.M., Chen, T.T., 2018. RNA-Seq analysis of differentially expressed genes relevant to innate and adaptive immunity in cecropin P1 transgenic rainbow trout (*Oncorhynchus mykiss*). BMC Genomics 19, 760.

Im, S.S., Yousef, L., Blaschitz, C., Liu, J.Z., Edwards, R.A., Young, S.G., Raffatellu, M., Osborne, T.F., 2011. Linking lipid metabolism to the innate immune response in macrophages through sterol regulatory element binding protein-1a. Cell Metab. 13, 540–549.

Jambeck, J.R., Geyer, R., Wilcox, C., Siegler, T.R., Perryman, M., Andrady, A., Narayan, R., Law, K.L., 2015. Plastic waste inputs from land into the ocean. Science 347, 768–771.

Kolpin, D.W., Furlong, E.T., Meyer, M.T., Thurman, E.M., Zaugg, S.D., Barber, L.B., Buxton, H.T., 2002. Pharmaceuticals, hormones, and other organic wastewater contaminants in US streams, 1999-2000: a national reconnaissance. Environ. Sci. Technol. 36, 1202–1211.

Kwon, J.W., Armbrust, K.L., 2006. Laboratory persistence and fate of fluoxetine in aquatic environments. Environ. Toxicol. Chem. 25, 2561–2568.

Li, J., Lusher, A.L., Rotchell, J.M., Deudero, S., Turra, A., Bråte, I.L.N., Sun, C., Hossain, M.S., Li, Q., Kolandhasamy, P., 2019. Using mussel as a global bioindicator of coastal microplastic pollution. Environ. Pollut. 244, 522–533.

Li, J., Yang, D., Li, L., Jabeen, K., Shi, H., 2015. Microplastics in commercial bivalves from China. Environ. Pollut. 207, 190–195.

Li, M., Qiu, L., Wang, L., Wang, W., Xin, L., Li, Y., Liu, Z., Song, L., 2016. The inhibitory role of γ-aminobutyric acid (GABA) on immunomodulation of Pacific oyster *Crassostrea gigas*. Fish Shellfish Immunol. 52, 16–22.

Liu, S., Shi, W., Guo, C., Zhao, X., Han, Y., Peng, C., Chai, X., Liu, G., 2016. Ocean acidification weakens the immune response of blood clam through hampering the NF-kappa β and toll-like receptor pathways. Fish Shellfish Immunol. 54, 322–327.

Liu, Z., Zhou, Z., Jiang, Q., Wang, L., Yi, Q., Qiu, L., Song, L., 2017. The neuroendocrine immunomodulatory axis-like pathway mediated by circulating haemocytes in pacific oyster *Crassostrea gigas*. Open Biol. 7, 160269.

Loker, E.S., Adema, C.M., Zhang, S.M., Kepler, T.B., 2004. Invertebrate immune systems - not homogeneous, not simple, not well understood. Immunol. Rev. 198, 10–24.

Lozoya, J., de Mello, F.T., Carrizo, D., Weinstein, F., Olivera, Y., Cedres, F., Pereira, M., Fossati, M., 2016. Plastics and microplastics on recreational beaches in Punta del Este (Uruguay): unseen critical residents? Environ. Pollut. 218, 931–941.

Lu, K., Qiao, R., An, H., Zhang, Y., 2018. Influence of microplastics on the accumulation and chronic toxic effects of cadmium in zebrafish (*Danio rerio*). Chemosphere 202, 514–520.

Livak, K.J., Schmittgen, T.D., 2001. Analysis of relative gene expression data using realtime quantitative PCR and the 2$^{-\Delta\Delta Ct}$ method. Methods 25, 402–408.

Marnett, L.J., 1999. Lipid peroxidation - DNA damage by malondialdehyde. Mut. Res. - Fund. Mol. M. 424, 83–95.

Melis, V., Usach, I., Peris, J.E., 2012. Determination of sertraline in rat plasma by HPLC and fluorescence detection and its application to *in vivo* pharmacokinetic studies. J. Sep. Sci. 35, 3302–3307.

Miller, T.H., Bury, N.R., Owen, S.F., MacRae, J.I., Barron, L.P., 2018. A review of the pharmaceutical exposome in aquatic fauna. Environ. Pollut. 239, 129–146.

Mogensen, S., Post, J.R., 2012. Energy allocation strategy modifies growth-survival tradeoffs in juvenile fish across ecological and environmental gradients. Oecologia 168, 923–933.

Nash, S.B., Dawson, A., Burkhard, M., Waugh, C., Huston, W., 2014. Detoxification enzyme activities (CYP1A1 and GST) in the skin of humpback whales as a function of organochlorine burdens and migration status. Aquat. Toxicol. 155, 207–212.

Ong, T.H.D., Yu, N., Meenashisundaram, G.K., Schaller, B., Gupta, M., 2017. Insight into cytotoxicity of Mg nanocomposites using MTT assay technique. Mat. Sci. Eng. C 78, 647–652.

Organisation for Economic Co-operation and Development, 2017. Health at a Glance2017: OECD Indicators. OECD Publishing, Paris.

Premanathan, M., Karthikeyan, K., Jeyasubramanian, K., Manivannan, G., 2011. Selective toxicity of ZnO nanoparticles toward Gram-positive bacteria and cancer cells by apoptosis through lipid peroxidation. Nanomedicine 7, 184–192.

Qu, H., Ma, R., Wang, B., Yang, J., Duan, L., Yu, G., 2019. Enantiospecific toxicity, distribution and bioaccumulation of chiral antidepressant venlafaxine and its metabolite in loach (*Misgurnus anguillicaudatus*) co-exposed to microplastic and the drugs. J. Hazard. Mater. 370, 203–211.

Razanajatovo, R.M., Ding, J., Zhang, S., Jiang, H., Zou, H., 2018. Sorption and desorption of selected pharmaceuticals by polyethylene microplastics. Mar. Pollut. Bull. 136, 516–523.

Repnik, U., Stoka, V., Turk, V., Turk, B., 2012. Lysosomes and lysosomal cathepsins in cell death. BBA - Proteins Proteom. 1824, 22–33.

Roberts, D.A., Birchenough, S.N., Lewis, C., Sanders, M.B., Bolam, T., Sheahan, D., 2013. Ocean acidification increases the toxicity of contaminated sediments. Global Change Biol. 19, 340–351.

Rochman, C.M., Hentschel, B.T., Teh, S.J., 2014. Long-term sorption of metals is similar among plastic types: implications for plastic debris in aquatic environments. Plos one 9, e85433.

Salgado, R., Marques, R., Noronha, J., Mexia, J., Carvalho, G., Oehmen, A., Reis, M., 2011. Assessing the diurnal variability of pharmaceutical and personal care products in a full-scale activated sludge plant. Environ. Pollut. 159, 2359–2367.

Sánchez-Argüello, P., Fernández, C., Tarazona, J.V., 2009. Assessing the effects of fluoxetine on *Physa acuta* (Gastropoda, Pulmonata) and *Chironomus riparius* (Insecta, Diptera) using a two-species water-sediment test. Sci. Total Environ. 407, 1937–1946.

Sarasquete, C., Segner, H., 2000. Cytochrome P4501A (CYP1A) in teleostean fishes. A review of immunohistochemical studies. Sci. Total Environ. 247, 313–332.

Schultz, M.M., Furlong, E.T., Kolpin, D.W., Werner, S.L., Schoenfuss, H.L., Barber, L.B., Blazer, V.S., Norris, D.O., Vajda, A.M., 2010. Antidepressant pharmaceuticals in two US effluent-impacted streams: occurrence and fate in water and sediment, and selective uptake in fish neural tissue. Environ. Sci. Technol. 44, 1918–1925.

Shi, W., Han, Y., Guan, X., Rong, J., Su, W., Zha, S., Tang, Y., Du, X., Liu, G., 2019. Fluoxetine suppresses the immune responses of blood clams by reducing haemocyte viability, disturbing signal transduction and imposing physiological stress. Sci. Total Environ. 683, 681–689.

Shi, W., Han, Y., Guo, C., Zhao, X., Liu, S., Su, W., Zha, S., Wang, Y., Liu, G., 2017. Immunotoxicity of nanoparticle nTiO$_2$ to a commercial marine bivalve species,

Tegillarca granosa. Fish Shellfish Immunol. 66, 300–306.

Silva, L.J., Pereira, A.M., Meisel, L.M., Lino, C.M., Pena, A., 2015. Reviewing the serotonin reuptake inhibitors (SSRIs) footprint in the aquatic biota: uptake, bioaccumulation and ecotoxicology. Environ. Pollut. 197, 127–143.

Sleight, V.A., Bakir, A., Thompson, R.C., Henry, T.B., 2017. Assessment of microplastic-sorbed contaminant bioavailability through analysis of biomarker gene expression in larval zebrafish. Mar. Pollut. Bull. 116, 291–297.

Su, W., Rong, J., Zha, S., Yan, M., Fang, J., Liu, G., 2018. Ocean acidification affects the cytoskeleton, lysozymes, and nitric oxide of hemocytes: a possible explanation for the hampered phagocytosis in blood clams, *Tegillarca granosa.* Front. Physiol. 9, 619.

Sussarellu, R., Suquet, M., Thomas, Y., Lambert, C., Fabioux, C., Pernet, M.E.J., Le Goïc, N., Quillien, V., Mingant, C., Epelboin, Y., 2016. Oyster reproduction is affected by exposure to polystyrene microplastics. P. Nalt. Acad. Sci. USA 113, 2430–2435.

Tang, Y., Rong, J., Guan, X., Zha, S., Shi, W., Han, Y., Du, X., Wu, F., Huang, W., Liu, G.,

2020. Immunotoxicity of microplastics and two persistent organic pollutants alone or in combination to a bivalve species. Environ. Pollut. 258, 113845.

Turvey, S.E., Broide, D.H., 2010. Innate immunity. J. Allergy Clin. Immun. 125, S24–S32.

Van Cauwenberghe, L., Claessens, M., Vandegehuchte, M.B., Janssen, C.R., 2015. Microplastics are taken up by mussels (*Mytilus edulis*) and lugworms (*Arenicola marina*) living in natural habitats. Environ. Pollut. 199, 10–17.

Van Cauwenberghe, L., Janssen, C.R., 2014. Microplastics in bivalves cultured for human consumption. Environ. Pollut. 193, 65–70.

Van Sebille, E., Wilcox, C., Lebreton, L., Maximenko, N., Hardesty, B.D., Van Franeker, J.A., Eriksen, M., Siegel, D., Galgani, F., Law, K.L., 2015. A global inventory of small floating plastic debris. Environ. Res. Lett. 10, 124006.

Yin, L., Chen, B., Xia, B., Shi, X., Qu, K., 2018. Polystyrene microplastics alter the behavior, energy reserve and nutritional composition of marine jacopever (*Sebastes schlegelii*). J. Hazard. Mater. 360, 97–105.